

# Sitka Spruce Quality Estimation using Neural Networks

D. O'Donoghue, J. Duffin, D. Hughes, J. G. Keating  
Department of Computer Science, St. Patrick's College Maynooth, Co. Kildare, Ireland.  
dodonoghue@vax1.may.ie

F. E. Feeney, V. Lawlor  
Computing, Physics and Mathematics Department, R.T.C. Carlow, Co. Carlow, Ireland.

J. Evertsen  
Forest Products Department, Forbairt, Ballymun Road, Glasnevin, Dublin 9, Ireland.

## ABSTRACT

This paper describes an automated classifier for the identification of good wood and knotty wood from computer tomography (CT) images of logs. Such a system is intended to allow better assessment of saw logs before being cut into timber. We describe a new empirical model for the growth of Sitka Spruce (*Picea Stichensis* (Bong, Carr)) whose operation is adapted to Irish conditions. The use of Hopfield networks for 2D cross-section image reconstruction from CT data obtained from the model is investigated. We also used a multi-layer feedforward neural network trained with fast-backpropagation to identify good wood from knotty wood. The Hopfield approach to image reconstruction was seen as being unsuitable for application with the wood industry. However, the use of a feedforward neural network for wood classification produced very promising results when trained on our tree model. It is expected that results from real wood data would be even more accurate.

## 1. INTRODUCTION

The quality of wood is currently assessed from its external appearance (Som, 1992). In this paper we present results from a investigations into the use of neural networks for automatic classification of good versus knotty wood using computer tomography (CT) data generated from an algebraic model of Sitka Spruce growth. This model is based on the Norway Spruce growth model of Kucera (1994) of wood density through a log section at various heights, in conjunction with empirical Irish data. Two formulae defining ring width and ring density for trees up to 55 years of age, form the basis of this model. As most trees in plantation forests are ready for felling at 50 years this seemed sufficiently accurate to test our classification system.

A two-stage (see Figure 1) neural network based classifier was investigated. The input network constructed cross-sectional images from tomographic data, and a classifying network identified knotty wood from them. Systems incorporating multiple stages of neural networks have already been used to model shape recognition Beiderman (1993) and to detect abnormal cervical cells McKenna (1992).

First, a Hopfield network was used for cross-sectional image reconstruction from modelled CT data for a variety of scan patterns and scan-beam densities in order to examine the effectiveness of a Hopfield image reconstruction technique to wood. The results for these experiments are presented and our conclusions discussed. Second, we used a multi-layer feedforward network trained with fast-backpropagation to segment cross-sections of wood, thus identifying regions which contain knots. As before, classification is based on image segments of model cross-sections. This model is discussed in some detail in the following section.

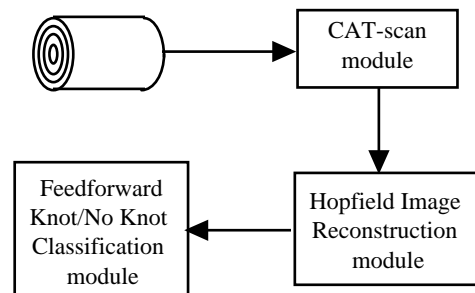


Figure 1 : Architecture of wood classification system.

## 2. AN EMPIRICAL MODEL OF TREE GROWTH

We developed a mathematical model of ideal Irish Sitka Spruce (*Picea Stichensis* (Bong, Carr)) growth adapted from an empirical model of Norway Spruce (Kucera (1994)) and Irish data (Evertsen (1986)). The

density of wood ( $d$ ) is dependent on the age ( $a$ ) of the ring from which that wood is taken, and is given by

$$d = 0.1437 * a^{0.242} + 1.100 * e^{-0.228 * a}$$

Timber from young wood is denser than that of old wood, and early wood (grown in Spring) denser than late wood. To compute the width of a ring ( $w$ ) we use the formula

$$w = -66.46 * a^{-1.444} + 7.816 * e^{-0.0209 * a}$$

where the width  $w$  is measured in millimetres. From this model we can generate a synthetic cross-section of an ideal tree. However, to train our classification network to identify knots we also wish to be able to model knotty wood. To do this we use the basic tree growth model, and apply it to branch growth within the tree. Branches are approximated by cones formed within the volume space of a tree trunk. This is an approximation as ring growth in the immediate vicinity of a knot is narrower than normal growth, thus forming contours around the knot.

To generate a sufficiently varied training set we model trees of different ages and heights, with branches emanating from the pith at different angles. Here our model of tree growth is specified by a 3-tuple  $T(A, L, B_i ; i=1, \dots, N)$  where  $A$  is the age of the trunk, and  $L$  the length of the trunk segment.  $B_i$  is a 3-tuple  $B_i(a_i, \phi_i, \theta_i)$  where  $a_i$  is the age of branch  $i$ ;  $\phi_i$  the branch's cardinal position, and  $\theta_i$  is the branch angle to the vertical (see Figure 2).

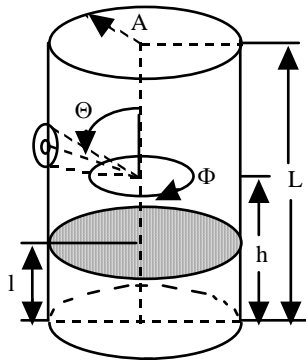


Figure 2 : Parameters describing model tree used to generate cross-sectional images.

Many different cross-sections can be generated from a single trunk model by taking cross-sections at different heights ( $l$ ). If  $l$  is less than the knot base height, the scan is that of the tree itself. Increasing  $l$  beyond  $h$  generates successive cross-sections where the knot increases in size and moves radially from the centre of the tree. At different sectional heights the dense knot wood may be surrounded by juvenile wood of variable density, adult wood of high density or a combination of these.

### 3. IMAGE RECONSTRUCTION

Computerised tomographic imaging is widely used in medicine and industry for generating cross-sectional images, and is typically performed in a manner similar to the CAT-scan image reconstruction technique developed by Hunsfield (1973). The image reconstruction process may be performed using an algebraic reconstruction technique (ART) (Kak and Stanley, 1988), a feedforward neural network trained using a filtered back-propagation algorithm (Floyd, 1991) or a modified recurrent Hopfield network (Srinivasan *et al*, 1993).

We have investigated the suitability of the method proposed by Srinivasan (1993) to the reconstruction of synthetic cross-sectional images of tree trunks. From our tree model we computed the attenuations suffered by beams of x-rays passing through the trunk of the tree (Lindgren, 1988). These attenuation figures formed the basis of the image reconstruction process, allowing calculation of the accuracy of the regenerated image by comparing it with the original model cross-section. The signal-to-noise ratio of the reconstructed image to the original is a measure of the technique's accuracy. The SNR is given by

$$SNR = 10 \log \left\{ \frac{\sum_{i=1}^N f_i^2}{\sum_{i=1}^N (f_{si} - f_i)^2} \right\}$$

where  $f_{si}$  and  $f_i$  are the attenuation coefficient of cell  $i$  for the actual and the reconstructed image respectively, and  $N$  the size of the image.

For the purposes of this paper it is assumed that the imaging system consists of an x-ray emitter-detector pair, that can be translated and rotated along various paths about the tree obtaining a variety of attenuation readings. By measuring beam attenuation and computing the path of these beams through the tree, we can compute the required weights and biases for the Hopfield network.

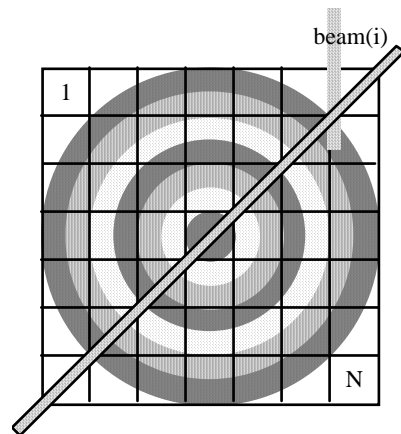


Figure 3 : Beam passing through cells of image area.

The image area is divided into an array of square cells (see Figure 3), each represented within the Hopfield network by a neuron whose output corresponds to the density for that image area. Each of the  $N$  cells covers an area  $A$ , with a constant attenuation coefficient  $f_i$ , and each beam is assumed to have a constant width  $\tau$  equal to the cell width. The total attenuation suffered by ray  $m$  is

$$\rho_m = \sum_{i=1}^N x_{mi} f_i$$

where  $x_{mi}$  is the area covered by beam  $m$  in cell  $i$ ;  $f_i$  is the output of neuron  $i$ . The input bias to cell  $i$  is calculated from the area covered by each beam intersecting that cell and the attenuation suffered by these beams, thus

$$I_i = 2 \sum_{m=1}^M x_{mi} \rho_m$$

where  $I_i$  is the input bias to cell  $i$ , and  $M$  is the total number of beams. Since the attenuation data is in the form of a single attenuation figure for each beam, the path followed by each beam through the image area must be determined.

Bresenham's line drawing algorithm was used to identify this path. This circumvented the calculation of partial intersection areas between beams and image cells, speeding up the computation of the input biases and weights of the artificial neurons. Since this is merely an approximation of the actual beam trajectory, it is accepted that this is a potential source of inaccuracy in the final reconstructed image.

From our results it seems that this approximation did not have a major impact on the accuracy of the reconstructed image, this being attributed to the fact that wood density (generally) varies gradually across the tree section (Lindgren *et al*, 1989). The use of Bresenham's algorithm means that  $x_{mi} = 1$  if beam  $m$  intercepts cell  $i$ , and 0 otherwise. The weights are calculated as follows

$$w_{ij} = -2 \sum_{m=1}^M x_{mj} x_{mi}$$

The dynamic behaviour of the network is governed by

$$u_i(t + \Delta t) = \left\{ \sum_{j=1}^N w_{ij} f_j(t) + I_i \right\} \Delta t + u_i(t)$$

where  $u_i$  is the input to neuron  $i$ ,  $N$  the total number of cells,  $f_i(t)$  is the output of neuron  $i$  at time  $t$ . From an initial state the neurons undergo a series of transitions,

reaching a final state corresponding to a minimum of the energy function.

$$E = \sum_{m=1}^M \sum_{j=1}^N \left( \sum_{i=1}^N x_{mi} x_{mj} f_i f_j - 2r_m x_{mj} f_j \right)$$

A modified version of this network (Srinivasan *et al.*, 1994) was implemented which required considerably fewer interconnections between neurons. A summation layer was introduced as follows

$$S_m = \sum_{i=1}^N x_{mi} f_i$$

The modified update function becomes

$$u_i(t + \Delta t) = \left\{ -2 \sum_{m=1}^M S_m x_{mi} + I_i \right\} \Delta t + u_i(t)$$

From our model a number of simulated attenuation readings were calculated for different scan patterns across the model tree. These attenuations were then used to generate the input biases and weights of the Hopfield network. The network was allowed to stabilise after which the output corresponds to densities in the reconstructed image. The accuracy of this reconstructed image was then compared with the original and the corresponding error calculated, using the formula for SNR above.

The following table shows the high ratio of beams to pixels required to construct an accurate image. This has the effect of slowing down the operation of the Hopfield network.

**Table 1 :** Correspondence between beams per pixel ratio and SNR.

Beams/pixel ratio	Signal/Noise ratio
0.37	10.82
0.45	11.00
0.51	12.50
0.73	12.02
0.85	21.36
0.97	31.72
1.04	35.4
1.16	106.6
1.42	109.6
1.61	117.4
1.84	125.8

It was found these results are better than those generally obtained using algebraic reconstruction techniques. However when larger amounts of tomographic data are collected, it was observed that there must be an even distribution of beams over the

surface of the image for this regeneration to succeed. It was found that in order to keep the error to an acceptable level the number of beams must approximately equal the number of image cells.

These results indicate that Hopfield networks should not be used with a single emitter-detector pair for CT image reconstruction, due to the excessive time taken to reconstruct wood and that radial scanning does not facilitate accurate image regeneration.

#### 4. KNOT IDENTIFICATION

The accurate detection of knots in wood is central to the production of good quality structural lumber from logs (Samson, 1993), the position and orientation of knots in lumber having a serious effect on the load carrying ability of wood. We present a method for the accurate identification of knots based on cross-sectional images of (simulated) logs, using a multi-layer feedforward neural network trained by fast-backpropagation (Samad, 1988).

Fast-backpropagation is a variant of the standard backpropagation algorithm, the only difference being that the error is added to the activation value prior to weight update. Thus

$$\Delta w_{ji}^{[s]} = \eta e_j^{[s]} (x_i^{[s-1]} + e_i^{[s-1]})$$

where  $\Delta w_{ji}^{[s]}$  is the change in weight connecting the  $i$ th neuron in layer  $(s-1)$  to the  $j$ th neuron in layer  $s$ ,  $\eta$  is a constant learning coefficient,  $e_j^{[s]}$  is the local error at neuron  $j$  in layer  $s$ ,  $x_i^{[s-1]}$  is the output of  $j$ th neuron in layer  $s$ .

A further refinement to this method adds a multiple of the error to the activation value

$$\Delta w_{ji}^{[s]} = \eta e_j^{[s]} (x_i^{[s-1]} + k e_i^{[s-1]})$$

where  $k = 1.0$  yields the unrefined fast-backpropagation update function above. Altering the value of  $k$  can produce a further increase in the learning rate.

In order to generate a neural network which segments the image into "knot" and "no knot" regions, pixels were randomly chosen from a series of images, and classified according to the density variation in a  $(2L + 1) \times (2L + 1)$  window about the pixel. Experiments showed that  $L = 3$  produced the most satisfactory results. The training data were taken from a variety of cross-sectional images associated with a trunk sample specified by a 30 year old tree with one branch at various angles to the vertical. Each window was classified as a "knot" or "no knot" region, forming the training set. Simulations were carried out using a 49-

25-1 feedforward network trained using fast-backpropagation.

In Table 2, test datum  $\underline{B}_0(10,180,45)$  showed relatively poor test results (85% success). This is due to the difference between this cross-section and those of the learning set. Adding this category to the learning set improved network performance.

**Table 2 :** Sample training sets and associated network performance.

No knots	$\theta$	1	% Success
1	70	130	60
1	70	130	72
2	70	120	89.25
3	60	150	89.25
4	45	170	97
4	70	170	85
4	70	140	90
5	70	140	95
6	70	140	95

Additional contour information in the immediate vicinity of a real knot leads us to believe that even better results could be expected from real wood data. This would be particularly useful for classifying the centre of a knot as opposed to classifying the pith of the tree itself.

#### 5. CONCLUSION

From the work described here we have reached two separate conclusions. The first is that a single emitter-detector pair in conjunction with reconstruction techniques based on Hopfield networks are not suitable for imaging in an industrial environment. This conclusion is based on both the time taken for the Hopfield network to execute, and the number of scans of the image area necessary to create a sufficiently accurate cross-section.

However, our results on the classification of wood quality are very encouraging. Training on just one cross-sectional image yielded a 72% detection rate when tested on different cross-sections. We expect that additional contour information from real wood samples would yield an even greater detection rate. Also, wood density can be greatly affected by such conditions as rot and wet wood. These are currently being included in our model tree, and their effects upon classification are under investigation.

#### ACKNOWLEDGEMENTS

The work on image reconstruction detailed in this paper was completed by J. Duffin in part fulfilment of

the Master of Computer Science requirements. Thanks are also due to J. Seery for his assistance with user interface programming.

## REFERENCES

Beiderman I, (1993) "Geon theory as an account of shape recognition in the mind and brain", AICS, Queens University Belfast, Northern Ireland, 7-17.

Kak A, Stanley M, (1988) Principles of Tomographic Imaging, IEEE press, New York.

Som S, Wells P, Davis J, (1992), "Automated feature extraction of wood from tomographic images", ICARCV'92 Second international conf. automation, robotics and computer vision, pp. 14.4.1 - 14.4.5.

Srinivasan V, Han Y K, Ong S H, (1993) "Image reconstruction by Hopfield network", Image and Vision Computing 11, 278 - 282.

Hunsfield, G. N. (1973) Computerised transverse axial scanning tomography. Br. J. Radio. 46, 1016.

McKenna s, Ricketts I, Cairns A, Hussein K, (1992) "Using a two-stage artificial neural network to detect abnormal cervical cells from their frequency domain image", Proceedings 2nd Irish Neural Networks Conference, Belfast Northern Ireland, June 25-26, 281-287.

Evertsen J, (1986) Determination of wood quality of standing trees by a non-destructive method. EC contract BO5-095-ER.

Floyd Jr C, (1991) An artificial neural network for SPECT image reconstruction, IEEE Trans. Medical Imaging 10, 485-487.

Hunsfield G, (1973) Computerised transverse axial scanning tomography, Br. J. Radio. 46, 1016.

Lindgren L. O. (1988) Non-destructive measurements and moisture content in wood using computerised tomography, Tech. Lic. Thesis, Royal Institute of Technology, Stockholm, Sweden.

Lindgren L. O., Lindberg H, Lindberg L. (1989) Calibration of a medical CAT-scanner for wood density and moisture content measurements, 5th Scandinavian Symposium on Materials Science, Copenhagen, May 22-25.

Lindgren L. O. (1991) Medical CAT-scanning; X-ray absorption coefficients, CT-numbers and their relation to wood density, Wood Sci. Technol. 25 341-349.

Mulligan F, (1986) A new technique for the real-time recovery of Fabry-Perot line profiles, J. Phys. E:Sci. Instrum. 19, 545-551.

Kulcera B (1994) A Hypothesis relating current annual height increment to juvenile wood formation in Norway Spruce, Wood and Fibre Science 26 (1), 156-167.

Samson M, (1993) Method for assessing the effect of knots in the conversion of logs into structural timber, Wood and Fiber Science 25 (3), 298-304.

Samad T, (1988), "Back-propagation is significantly faster if the expected value of the is used for update", International Neural Networks Conference Abstracts.